AAPS PharmSciTech (2022) 23: 182
https://doi.org/10.1208/s12249-022-02337-2

RESEARCH ARTICLE

Clove Oil Endorsed Transdermal Flux of Dronedarone Hydrochloride Loaded Bilosomal Nanogel: Factorial Design, In vitro Evaluation and Ex vivo Permeation

Mahmoud H. Teaima[1] · Jihad Mahmoud Alsofany[2] · Mohamed A. El-Nabarawi[1]

Received: 14 April 2022 / Accepted: 20 June 2022 / Published online: 1 July 2022

Abstract

The goal of this study was to develop a bilosomal gel formulation to enhance transdermal permeability of dronedarone hyrdrochloride (DRN) which suffers from poor oral absorption and limited bioavailability. To overcome this obstacle, bilosomes were successfully prepared using 2^3 full-factorial design. Span®40, cholesterol, sodium deoxycholate (bile salt), clove oil (permeability enhancer), and either Tween® 60 or Tween® 80 (edge activator) were used in bilosome preparation by ethanol injection method. In this design, independent variables were X1, edge activator type; X2, edge activator amount (mg); and X3, permeability enhancer concentration (% w/v). Optimal formula (B2) of the highest desirability of (0.776) demonstrated minimum vesicle size (VS) of 312.4 ± 24.42 nm, maximum absolute value of zeta potential (ZP) − 36.17 ± 2.57 mV, maximum entrapment efficiency (EE %) of 80.95 ± 3.01%, maximum deformability Index (DI) of 8.24 ± 1.26 g and maximum drug flux after 12 h (J_{12}) of 21.23 ± 1.54 μg/cm^2 h upon ex vivo permeation study. After 12 h, 70.29 ± 6.46% of DRN was released from B2. TEM identification of B2 showed spherical shaped nanosized vesicles which were physically stable for 3 months at different temperatures. B2 was incorporated into carboxymethylcellulose gel base for easiness of dermal application. B2 gel demonstrated good physical properties, non-Newtonian psuedoplastic flow, and enhanced release (57.0 ± 8.68% of DRN compared to only 13.3 ± 1.2% released from drug suspension after 12 h) and enhanced skin permeation.

Keywords Bilosome · Dronedarone · Transdermal · Nanovesicle · Gel

Introduction

Dronedarone hydrochloride (DRN) is a new agent in class III antiarrhythmic drug that has been officially approved by FDA in 2009 for the treatment of atrial fibrillation (type of heart arrhythmia) analogous to amiodarone but with less side effects [1–3]. DRN suffers from poor oral bioavailability which is an outcome of extensive first-pass metabolism, low solubility, and reduced absorption in the gastrointestinal tract [3, 4]. The reported absolute bioavailability of the tablet dosage form of DRN (Multaq®, Sanofi) in fasted state is only about 4%, while it reaches about 15% when it is administered with a high-fat meal in healthy volunteers [3, 4]. The solubility of DRN is pH dependent which reach about 1–2 mg/mL, at pH 3–5, while it significantly decreases in both gastric fluid (pH 1.2) and intestinal fluid (pH 6.8) [3, 4].

Skin has gained enormous attention as a route of drug delivery by pharmaceutical researchers. Transdermal drug delivery is defined as the topical application of drug onto the skin to be absorbed and cross skin barrier to reach systemic circulation through the beneath capillary network [5]. Transdermal delivery is more advantageous over conventional methods for drug delivery due to ease of accessibility, high safety, improved patient compliance, avoidance of fluctuating blood levels of drug after oral, or injectable therapy by providing steady drug level into blood stream

✉ Mahmoud H. Teaima
mahmoud.teaima@pharma.cu.edu.eg

Jihad Mahmoud Alsofany
jihad.alsofany@fop.usc.edu.eg

Mohamed A. El-Nabarawi
mohamed.elnabarawi@pharma.cu.edu.eg

[1] Department of Pharmaceutics and Industrial Pharmacy, Faculty of Pharmacy, Cairo University, Cairo, Egypt

[2] Department of Pharmaceutics and Industrial Pharmacy, Faculty of Pharmacy, University of Sadat City, Sadat City, Monufia, Egypt

over an extended period of time [6]. Additionally and most importantly, transdermal route is ideal for drugs suffer from first-pass metabolism when administered orally which is the main hurdle that limits DRN oral bioavailability [7]. Several previous formulation approaches to enhance DRN solubility, oral absorption, and oral bioavailability have been reported such as preparation of DRN complexes [8, 9], DRN entrapment into proliposomes [10], formulation of solid dispersions [3], entrapment into solid lipid nanoparticles [2], and formulation of self micro-emulsifying drug delivery systems [4]. The previous studies focused mainly on improvement of oral bioavailability.

Bilosomes first emerged in 2001 by Conacher et al. [11] who introduced the term (bilosomes) after their work on oral immunization made of bovine serum albumin as a standard antigen, a synthetic measles peptide and an influenza subunit vaccine. This formulation was successfully entrapped into lipoid non ionic surfactant vesicles and stabilized by bile salts. Bilosomes are nanovesicular lipid carriers consist of deoxycholic acid incorporated into the membrane of niosomes [11]. They are developed from natural lipids; therefore, they are biocompatible. Embedding of bile salts amplify vesicle elasticity [12] and enhance drug absorption and transportation through biological membranes including buccal, skin, intestinal, corneal, and blood–brain barrier [13]. Penetration enhancement mechanism of bile salts involves increasing the solubility of lipophilic drugs and boosting the fluidity of both the apical and basolateral membranes [14, 15]. Bilosomes are superior to conventional liposomes and niosomes due to their greater flexibility, elasticity, and deformability [16]. Bilosomes was extensively scrutinized for transdermal/cutaneous delivery of drugs such as lornixicam [17], dapsone [13], diacerein [18], and tenoxicam [19].

In the current study, the potential of bilosomes as novel nanovesicular carrier for the transdermal delivery of DRN will be explored. The rationale behind our study is to bypass gastric metabolism of DRN for improvement of its solubility and permeability across the skin and consequently enhancement of its absorption into systemic circulation. As mentioned earlier, DRN absorption is chiefly dependent on patient diet, *i.e.*, absorption increased with high fat meat, so the amount of DRN absorbed and hence its bioavailability is extremely variable upon oral administration. The erratic absorption and bioavailability will pessimistically influence DRN therapeutic outcomes. In this regard; transdermal route was chosen in our study to solve the problem of food-dependent absorption and poor oral bioavailability. Based on a profound literature review, DRN has not been investigated so far for potential transdermal delivery to solve the problem of poor oral bioavailability. Most of previous reported studies focused on improvement of DRN solubility and dissolution rate to improve its oral bioavailability as mentioned before. In the current study, the impact of different formulation variables (independent variables) on the characters of DRN-loaded bilosomes will be investigated using a full-factorial design 2^3. Design Expert software® will be used for data analysis and optimization of DRN-loaded bilosomes. The solid state of DRN in the optimized bilosomes will be examined using differential scanning calorimetry (DSC). The release profile and capability of the optimal DRN-loaded bilosomes to traverse rats' skin layers will be investigated in vitro and compared to that of free DRN aqueous suspension. Finally, optimal formula of DRN-loaded bilosomes will be incorporated into carboxymethylcellulose gel base for the ease of skin application. The rheological behavior, viscosity, release profile, skin deposition, and skin permeability of the prepared bilosomal gel will be studied to anticipate the drug ability to traverse skin barrier.

Materials and Method

Materials

Dronedarone hydrochloride (DRN), purity: 100.1% w/w, on anhydrous basis (Glenmark Generics Limited, India) was kindly gifted from Al-Andalus pharmaceutical company, Egypt. Cholesterol (CH) (Sigma-Aldrich, USA). Span® 40 (Oxford Lab chem, Mumbai, India). Tween® 60 (T60) (Acros Organic, USA). Tween® 80 (T80) (El Nasr pharmaceutical chemicals company, Cairo, Egypt). Sodium deoxycholate (SDC) (SD Fine Chemicals India). Clove oil (Sigm-Aldrich, USA). Sodium carboymethylcellulose (Na CMC) (SINOCMC, Qingdao, China), sodium chloride, potassium chloride, sodium phosphate dibasic, potassium dihydrogen phosphate, and ethanol absolute (El Gomhoriyah chemical company, Cairo, Egypt). Nylon filters 200 nm pore size (Sterlitech, Washington, USA). Cellulose dialysis membrane 12.000–14.000 M.wt cutoff (SERVA electrophoresis, Heidelberg, Germany).

Preparation of DRN-Loaded Bilosomes

Span® type (Span® 40), Span® to cholesterol ratio (1:1) and sodium deoxycholate concentration (0.2% w/v) were chosen for this study according to a previous screening study to select the optimal Span® type and concentration and optimal bile salt concentration that give minimum vesicle size (VS), minimum polydispersity index (PDI), maximum zeta potential (ZP), and maximum entrapment efficiency (EE%) (data not shown).

Bilosomes were prepared by ethanol injection method [20]. Simply; the surfactant (Span® 40), cholesterol (CH), clove oil, and drug (DRN) were first dissolved in organic solvent (10 mL ethanol). The prepared organic phase was then

injected dropwise into preheated 10 mL distilled water containing 0.2% (w/v) bile salt (SDC) and edge activator (T60 or T80) through fine injection needle connected to injection pump at fixed rate (20 drops/min). The mixture was then magnetically stirred using Hotplate Magnetic stirrer MS-H550-Pro (Medfuture Biotech CO, China) at fixed rotation rate and maintained at 65°C for 2 h. Stirring was continued until all ethanol evaporated to get drug-loaded bilosomes. This dispersion was sonicated for 15 min to reduce vesicle size of any aggregates using bath sonicator (Crest Ultrasonics Corp., NJ, USA) and stored at 2–8°C until further use.

Evaluation of the Prepared DRN-Loaded Bilosomes

Vesicle Size, Size Distribution, and Zeta Potential

VS, size distribution represented by polydispersity index (PDI), and zeta potential (ZP) of the prepared DRN vesicles were measured using Zetasizer Nano ZS-90 instrument (Malvern instruments, southboro, MA, USA). An aliquot of the dispersion was diluted before the measurement. Measurements were performed in triplicate using 90° scattering angle at 25°C, dispersant viscosity at 0.8872 cP and dielectric constant at 78.5. The displayed results are the mean value ± standard deviation.

Entrapment Efficiency (EE %)

The EE% of DRN-loaded bilosomes was determined indirectly by calculating the difference between the total amount of DRN incorporated into formulation and the amount remained in the supernatant after separating the prepared vesicles by centrifugation at 15,000 rpm for 1 h at 4°C using cooling centrifuge (Hermle Z326K, Labortechnik GmbH, Germany). The concentration of free DRN was measured spectrophotometrically by measuring the ultraviolet (UV) absorbance (Evolution 201 UV–visible spectrophotometer, Thermo Scientific, Massachusetts, USA). Drug EE% was calculated according to the following equation [21]:

$$EE\% = \frac{\text{Total amount of DRN} - \text{Free amount of DRN}}{\text{Total amount of DRN}} \times 100 \quad (1)$$

Measurement of Vesicle Elasticity (Deformability Index)

Measurement of vesicle elasticity represented by deformability index (DI) was performed by extruding bilosomal dispersion through nylon filters of 200 nm pore size [22, 23] under a pressure of 2.5 bar using air compressor. The expression of vesicular membrane elasticity in terms of deformability index (DI) was according to the following equation [24]:

$$DI = J\left(\frac{rv}{rp}\right)^2 \quad (2)$$

where J is the weight of the sample (g) extruded in 10 min, rv is the size of the vesicles after extrusion (nm), and rp is the pore size of the nylon filter (nm).

Ex vivo Permeation Study

The permeation capacity of DRN-loaded bilosomal dispersion *vs.* free DRN aqueous suspension was evaluated ex vivo using rat's skin. The study was approved by the ethical board of the Faculty of Pharmacy, Cairo University (PI 2785). The utilization and handling of animals complied with the EU directive 2010/63/EU. Removal of rat's skin was done following sacrifice of animals. Amount of bilosomal dispersion and aqueous suspension equivalent to 20 mg DRN were added in plastic cylindrical tubes with fixed permeation area that have one end firmly enclosed with a rat's skin (skin was immersed overnight in release medium before experiment). The other end was attached to the shaft of the USP dissolution apparatus (substituting baskets' position for 12 h at 37 ± 0.5°C). Tubes containing bilosomal dispersions were immersed in 100 mL PBS pH 7.4 containing ethanol (3:2) to maintain sink condition. Sampling was performed at 0.5, 1, 2, 3, 4, 5, 6, 7, 8, 9, 10, 11, and 12 h time intervals and analyzed spectrophotometerically by measuring UV absorbance. Permeation profiles of different formulae were represented by plotting the cumulative amounts of DRN permeated per unit area (Q) (μg/cm^2) against time (h). The average flux (J) (μg/cm^2 h) was the slope of the linear regression line of the permeation profile [25, 26]. Enhancement ratio (ER), which is the ratio of drug average drug flux from formula to average flux of free drug suspension was also calculated. Experiments were done in triplicate and the results represented as mean ± SD.

Factorial Experimental Design 2^3 of the Study

A 2^3 full-factorial design was implemented to estimate the influence of different formulation variables on the properties of DRN-loaded bilosomes by the aid of Design-Expert® software (version 7, Sat-Ease, Inc., Minneapolis, MN). Experimental trials were performed with all possible combinations for formulation of DRN-loaded bilosomes. The design is summarized in Table 1.

Selection and Validation of the Optimal DRN-Loaded Bilosomes

Desirability function was the tool used for the choice of optimal formula with the least VS, highest ZP (absolute value), highest DI, and highest flux (J_{12}). Optimal formula

Table 1 Factorial experimental design $2.^3$ of DRN-loaded bilosomes

Independent variables (factors)	Constrains	
X1: EA type	T60	T80
X2: EA amount (mg)	25	50
X3: PE concentration (% w/v)	1.5	3
Dependent variables (responses)	Constrains	
Y1:VS (nm)	Minimize	
Y2: ZP (mV)	Maximize	
Y3: DI (g)	Maximize	
Y4: J_{12} (μg/cm^2 h)	Maximize	

of greatest desirability value was prepared, characterized and correlated to the predicted responses using Design-Expert® Software (version 7, Stat-Ease Inc., Minneapolis, MN, USA).

TEM

The optimal formula was morphologically photographed by transmission electron microscopy (TEM) (JEOL RI 2100, Germany). Stained bilosome sample was placed on a carbon grid with copper coat and kept to dry until formation of thin film. The sheet of copper was positioned inside the TEM.

In vitro Release Study of the Selected Formula

Release of DRN from bilosomal dispersion of the optimized formula *vs.* free drug suspension was scrutinized. Amount of DRN bilosomal dispersion equivalent to 20 mg DRN was added into plastic cylindrical tubes with fixed permeation area that have one end tightly enclosed with a dialysis membrane (membrane was immersed overnight in release medium before experiment). The other end connected to the shaft of the USP dissolution apparatus substituting baskets' position for 12 h at 37 ± 2°C. Tubes containing DRN bilosomal dispersion and free drug suspension were immersed in 100 mL 100 mL PBS pH 7.4 containing ethanol (3:2) to maintain sink condition. Sampling was performed every 1-h time interval and up to 12 h. Samples were measured spectrophotometerically by measuring maximum UV absorbance. Release profiles of tested samples were represented by plotting the % cumulative amounts of DRN released against time (h). Experiments were done in triplicates and results are represented as mean ± SD.

Lyophilization of the Optimized DRN-Loaded Bilosomes

The optimized formula was lyophilized after preparation. DRN bilosomes dispersion was pre-frozen at − 80°C (ultralow temperature freezer, so-low, ultra-low freezer, Environmental Equipment Cincinnati, Ohio, USA) for 24 h, and the samples were freeze-dried using freeze dryer (Bondiro Freeze Dryer, IIshin Lab Co Ltd, Korea).

DSC

Five milligrams from DRN powder and lyophilized optimal formula were subjected to thermal analysis using DSC (DSC-60, Shimadzu Corp., Kyoto, Japan) in a temperature range of 10–400°C at a scanning rate of 10°C/min under inert nitrogen flow (25 mL/min) standardized with purified indium.

Stability Study of the Optimal Formula

The optimal DRN-loaded bilosomes formula was stored at 4°C and 25°C for 90 days. Samples from each formulation were taken at 0 and 90 days. Stability was anticipated by assessment of VS, PDI, ZP, and EE% (as mentioned earlier) at zero time relative to results obtained after 90 days of storage [27]. Statistical significance was analyzed by ANOVA test using SPSS® software version17.0 (SPSS, Chicago, IL, USA). Difference at $P \leq 0.05$ was considered significant.

Formulation of DRN Bilosomal Gel

One percent (w/v) NaCMC was weighed and added to the optimal DRN-loaded bilosome dispersion and mixed thoroughly using magnetic stirrer till formation of homogenous gel.

Evaluation of DRN Bilosomal Gel

Visual Examination and pH Measurements

The prepared DRN-loaded bilosomal gel was examined visually for color, homogeneity, and phase separation of gel system. The pH value of the prepared DRN-loaded bilosomal gel was determined using a pH meter (MEDFUTURE 920 precision PH/ORP meter, Medfuture Biotech CO, China).

Viscosity Measurements and Rheological Properties

The viscosity values of the prepared DRN bilosomal gel were measured with a rotational type rheometer (Brookfield Digital Rheometer type DV III, Brookfield Engineering, USA). The shear stress formed under different shear rate conditions (rpm increasing from 0.5 to 5 and decreasing from 5 to 0.5) on the formulation was measured using CPE-40 spindle. The temperature was set to 25 ± 2°C, and the viscosity values of the gel were measured. Finally, the flow properties of the gel were determined by plotting the shear rate against the shear stress. The obtained data were fitted

to the power-law model to predict the rheological behavior of the formed gel:

$$\tau = k\gamma^n \quad (3)$$

where τ is the shear stress (dyne/cm^2), k is the consistency index (dyne/cm^2 sn^2), γ is the shear rate (/s), and n is the index of flow.

In vitro Release Study of DRN-Loaded Bilosomal Gel

Release study of the prepared gel was carried out as described before. Release profile of the gel was plotted and compared to both bilosomal dispersion and drug suspension profiles.

Ex vivo Permeation Study of DRN-Loaded Bilosomal Gel

The permeation potential of DRN-loaded bilosomal gel across rats' skin was evaluated as mentioned earlier.

Ex vivo Skin Deposition Study of DRN-Loaded Bilosomal Gel

At the end of the skin permeation experiment, skin samples were removed and cleaned with cotton soaked in phosphate buffer for three times to remove any remaining gel. Skin was then separated into three different layers using tape-stripping technique for the stratum corneum [28] and forceps to separate the dermis from epidermis. Each layer was extracted using absolute methanol to ensure the complete extraction of any retained drug. The skin extracts were then sonicated for 30 min and filtered using 0.22 µ membrane filters and injected into the HPLC for the quantification of the drug content. An isocratic reversed-phase validated HPLC method was used for detection and quantification of DRN using an Agilent 1260 Infinity LC system equipped with quaternary pump, an auto-sampler unit, and a UV detector. The stationary phase was Inertsil ODS (4.6 × 250 mm, 3.5 µm) column packed with a 5-µm-size adsorbent. Mixture of deionized water (containing 1 ml triethylamine pH 2.3 adjusted with orthophosphoric acid)/acetonitril (49:51 v/v) was used as mobile phase at 1 mL/min flow rate. The detector was set at 290 nm, and the injection volume was 20 µL. The skin deposition amount of DRN was calculated from the obtained data. Following the experiment, incineration was done for the destruction of animal carcasses. Experiment was done in triplicate and results are represented as mean ± SD.

Results and Discussion

Analysis of Factorial Design

Factorial designs permit simultaneous analysis of the effect of different variables on the characteristics of the drug formulation. Desirability function is an effective means for defining the optimal levels of the variables. The 2^3 design statistics are summarized in Table 2.

Effect of Variables on VS

Vesicle size is a fundamental variable for formulation and optimization of nanovesicles intended for transdermal delivery. Smaller vesicles have higher potential to traverse skin deeper than larger ones [29]. Vesicle size measured for the prepared DRN-loaded bilosomes ranged from 146.20 ± 0.90 nm for B5 to 360.2 ± 5.87 nm for B3. PDI values of all formulae laid between 0.23 ± 0.01 for B5 and 0.54 ± 0.01 for B2 which is considered an acceptable results [30]. PDI is preferred to be less than 0.3 but values less than 0.7 are still acceptable because different size distribution

Table 2 The model summary statistics of 2^3 full-factorial design used for optimization of DRN-loaded bilosomes

Responses	Y1: VS (nm)	Y2: ZP (mV)	Y3: DI (g)	Y4: J_{12} (µg/cm^2 h)
Minimum	145.2	− 20.4	1.74	4.28
Maximum	412.9	− 39.1	14.94	22.53
Ratio	2.84	1.92	8.59	5.26
Model	2FI	2FI	2FI	Cubic
adequate precision	17.81	18.65	14.62	21.4
R^2	0.91	0.93	0.87	0.95
Adjusted R^2	0.88	0.91	0.82	0.92
Predicted R^2	0.82	0.87	0.74	0.88
Significant factors	X1,X3	X1,X2,X3	X1,X3	X1,X2,X3
Predicted values of optimum formula (B2)	318.03	− 35.52	8.2	21.23
Observed values of optimum formula (B2)	312.43	− 36.17	8.24	21.23
% Bias	1.8	1.8	0.49	0

algorithms work with data that fall between PDI range (0.05–0.7) [31]. If the value goes beyond 0.7, the sample cannot be analyzed by dynamic light scattering method [32]. Results are summarized in Table 3.

ANOVA testing for vesicle size model resulted in *P* value < 0.05 which indicates that the model terms are significant. In this model, X1 (EA type) and X3 (PE conc.) are significant model terms. Concerning EA type (X1), T60 resulted in significantly smaller vesicle size than that obtained by T80 (Fig. 1). This could be ascribed to the lower hydrophilicity of T60 compared to T80. Edge activator of a lower HLB resulted in decreasing the surface free energy and formation of nanovesicles with a smaller size [33]. These findings are in agreement with Mazyad et al. [34] who reported that T60-based spanlastics were smaller in size than those based on T80. Ruckmani and Sankar [35] also achieved the same results upon their work on zidovudine niosomes. They noticed that the vesicle size increases as the hydrophilicity of the nonionic surfactant increases. Increasing amount of PE (clove oil) resulted in increased vesicle size. This could be a result of aggregation of bilosomes due to the high level of utilized lipids. Our findings are similar to those reported by Elsayed et al. [32] and Hao and Li [36].

Effect of Variables on ZP

Zeta potential is the measure of the entire charges gained by nanovesicles, and it is considered as a tool for stability evaluation of colloidal dispersions, the higher the ZP values, the higher the repulsion forces that prevent the nanovesicle aggregation [37]. All formulae showed acceptable ZP values ranged from − 20.83 ± 0.51 mV for B8 to − 37.43 ± 1.50 mV for B3 demonstrating that the DRN-loaded bilosomes acquired enough charges that would hinder their aggregation. The negative ZP of bilosomes was originated from the anionic SDC (deoxycholate anion). In addition, the partial hydrolysis of polyethylene oxide head groups of Tweens® contributed to the observed negative charge despite being nonionic surfactants [38, 39]. ANOVA testing revealed a significant impact of all the examined factors (X1, X2, and X3) on the measured ZP as confirmed by *P* values < 0.05. T60 resulted in higher absolute value of ZP than that obtained by T80. Having saturated alkyl chain structure; T60 put across certain rigidity to the formed lipid layer of bilosomes which increased its stability and hence zeta potential. Dissimilar to T80 which have an unsaturated alkyl chain that permits it to bend and resulted in more permeable less stable vesicles [25, 40].

Increasing concentration of EAs resulted in lowering ZP value (Fig. 1). This may be explained by the fact that EAs tend to reside on the surface of the vesicular bilayers because they have certain hydrophilic characters as reported by Wilson et al. [41]. As a result shielding of the surface charge

Table 3 Experimental runs, independent variables, and measured responses of the 2^3 full-factorial experimental design of DRN-loaded bilosomes

Formula	EA type	EA amount (mg)	PE (% w/v)	VS (nm)	PDI	ZP (mV)	EE %	DI (g)	Q10 (μg/cm^2)	J_{12} (μg/cm^2 h)	ER
B1	T60	25	3	254.73 ± 2.50	0.43 ± 0.15	− 34.90 ± 1.71	81.22 ± 2.30	5.54 ± 0.11	201.77 ± 11.50	13.40 ± 0.33	2.03
B2	T60	50	3	312.43 ± 24.42	0.54 ± 0.01	− 36.17 ± 2.60	80.95 ± 3.01	8.24 ± 1.26	349.66 ± 20.60	21.23 ± 1.54	3.2
B3	T80	25	3	360.20 ± 5.87	0.46 ± 0.01	− 37.43 ± 1.50	80.16 ± 5.95	11.49 ± 3.00	222.18 ± 33.02	15.10 ± 2.21	2.3
B4	T80	50	3	306.07 ± 12.40	0.38 ± 0.03	− 32.33 ± 2.50	79.99 ± 7.68	7.93 ± 0.65	202.45 ± 13.76	13.51 ± 1.83	2.05
B5	T60	25	1.5	146.20 ± 0.90	0.23 ± 0.01	− 34.10 ± 1.65	73.27 ± 2.82	1.76 ± 0.02	143.81 ± 11.04	11.62 ± 1.10	1.76
B6	T60	50	1.5	252.50 ± 19.83	0.42 ± 0.06	− 26.83 ± 0.67	81.03 ± 3.75	5.29 ± 0.84	131.43 ± 8.14	10.83 ± 0.89	1.64
B7	T80	25	1.5	314.20 ± 4.70	0.38 ± 0.02	− 28.60 ± 1.31	75.22 ± 5.13	8.16 ± 0.24	73.47 ± 12.03	5.10 ± 0.81	0.77
B8	T80	50	1.5	263.90 ± 23.65	0.39 ± 0.04	− 20.83 ± 0.51	80.16 ± 2.92	5.79 ± 1.05	101.50 ± 9.80	7.82 ± 0.56	1.2

Data represented as mean ± SD ($n = 3$)

X1 EA type, *X2* EA amount, *X3* PE concentration, $Y_1(VS)$ vesicle size (nm), $Y_2(ZP)$ zeta potential (mV), $Y_3(DI)$ deformability index (g); $Y_4(J_{12})$ drug flux after 12 h (μg/cm^2 h), *EE%* entrapment efficiency percent (%), *PDI* polydispersity index, *Q10* cumulative amount DRN permeated per unit area after 10 h (μg/cm.^{2}), *ER* enhancement ratio

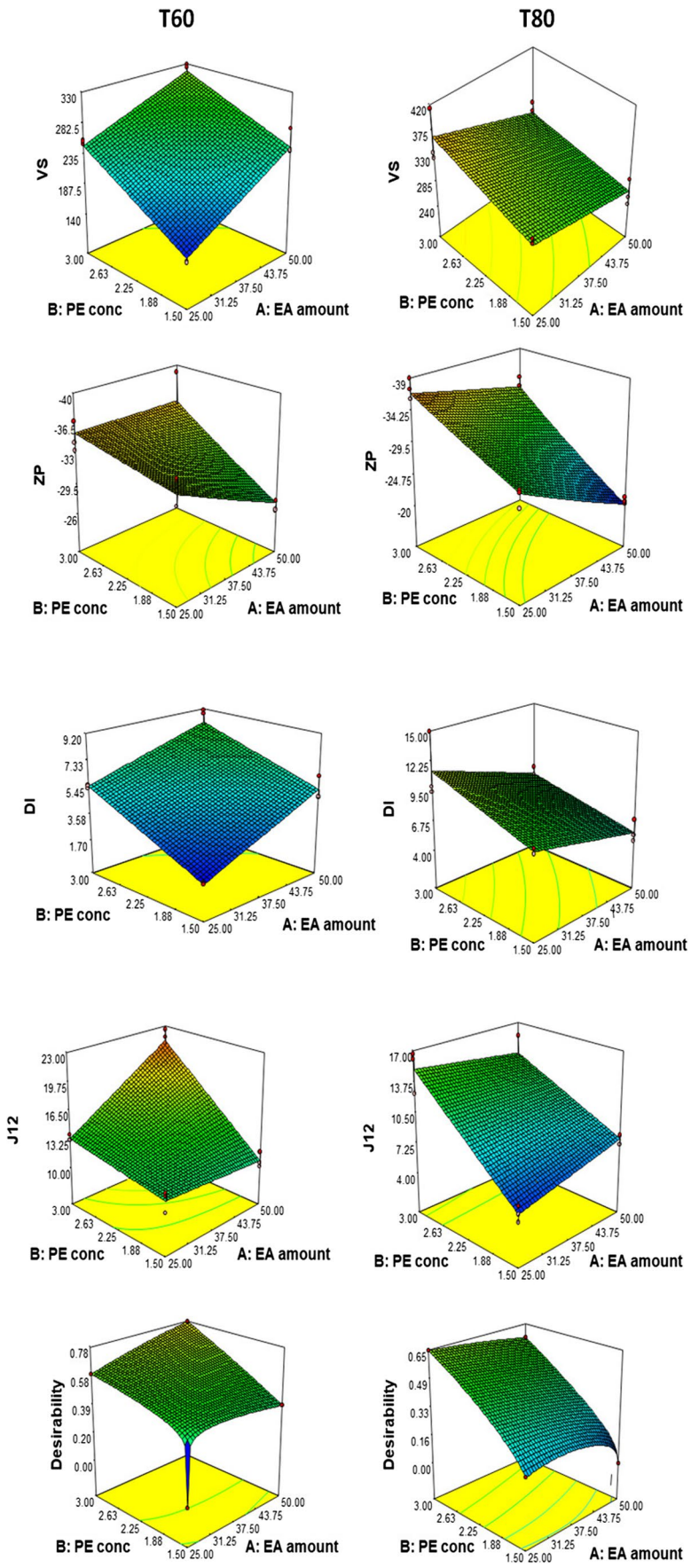

Fig. 1 Response surface plot for the effects of EA amount (X2) and PE concentration (X3) on vesicle size (VS), zeta potential (ZP), deformability index (DI), average flux (J_{12}), and desirability of DRN bilosome formulae loaded with either T60 or T80 as an edge activator (X1)

occurred by EA presence on the vesicle surface [42]. Higher concentration of PE (clove oil) gave more stable vesicles with higher ZP values. This could be attributed to the negative charge added by eugenol which is the main constituent of clove oil. Our finding is in harmony with Xu et al. [43] who detected increased zeta potential of eugenol-casein nanoparticles upon increasing concentration of eugenol.

Effect of Variables on DI

Deformability index is a measure of vesicles elasticity. Elasticity facilitates nanovesicles penetration through the skin layers and decreases the possibility of their rupture while squeezing [20]. The measured DI values of DRN bilosome formulae ranged from 1.76 ± 0.02 for B5 to 11.49 ± 3.00 for B3. X1(EA type) and X3 (PE conc.) were statistically significant model terms. Regarding EA type (X1), bilosomes formulated using T80 as EA gained higher DI than those formulated using T60. This result comes in agreement with that obtained by Elsayed et al. [32] who noticed that increasing T80 gave significantly more elastic rosuvastatin loaded nanovesicles with minor size change. Our results are also in harmony with that declared by Van den Bergh et al. [44] upon their work to develop elastic vesicles composed chiefly of non-ionic surfactant like T80. Another possible explanation is that bilosomes prepared by T80 were of larger size than those prepared by T60 and vesicle size is directly proportional to DI; thus, DI is higher for T80-based bilosomes. Increasing PE concentration (X3) resulted in significant increase in DI value. This may be a result of increased vesicle size because of the high level of utilized lipids [45]. Bilosomes of larger size that could squeeze in through nanosized filter pores (200 nm) were those of higher elasticity and deformability index. According to the equation mentioned earlier, DI is directly proportional to vesicle size. Results are illustrated in Fig. 1 and Table 3.

Effect of Variables on Average Flux (J_{12})

Permeation profiles are shown in Fig. 2. Cumulative amount of DRN permeated per unit area of rats' skin in vitro after 10 h (Q_{10}) drug average flux after 12 h (J_{12}) and enhancement ratio (ER) are represented in Table 3. All formulae prepared with 3% clove oil (PE) showed significantly higher permeation parameters, *i.e.*, Q_{10}, J_{12} and ER than those prepared with 1.5% clove oil ($P < 0.05$), which reflects the principal role of clove oil concentration in augmenting DRN skin penetration.

All the three independent variables (X1, X2, and X3) affected average flux value (J_{12}) significantly. For EA type (X1), the average flux after 12 h (J_{12}) of DRN-loaded bilosomes prepared by T60 as an EA was higher than those prepared by T80. As discussed earlier, the stable saturated alkyl chain of T60 impart certain rigidity and stability to the formed bilosomes which prevent entrapped drug from escaping outside nanovesicles and consequently enhance drug flux and permeation across skin [25, 40]. In opposition, the unsaturated alkyl chain of T80 permits its twisting at the surface of bilosomes rendering nanovesicles into less stable more permeable which allows drug flee from nanovesicles and subsequently less skin permeation attained [25, 40]. Additionally, T60-based bilosomes were significantly smaller in size than T80 based; hence, the permeation of smaller bilosomes through narrow skin pores was more efficient.

Increasing EA content (X2) boosted up flux value (J_{12}) significantly. Tweens® as EAs are nonionic surfactants containing ethylene oxide and a long alkyl chain that possess both hydrophilic and hydrophobic properties. This dual feature allows the partitioning of DRN bilosomes between both lipophilic lipid domain and hydrophilic protein domain of stratum corneum. Subsequently, drug flux and skin penetration enhanced. In general, nonionic surfactants are safer, less toxic, and less skin irritant compared to anionic, cationic,

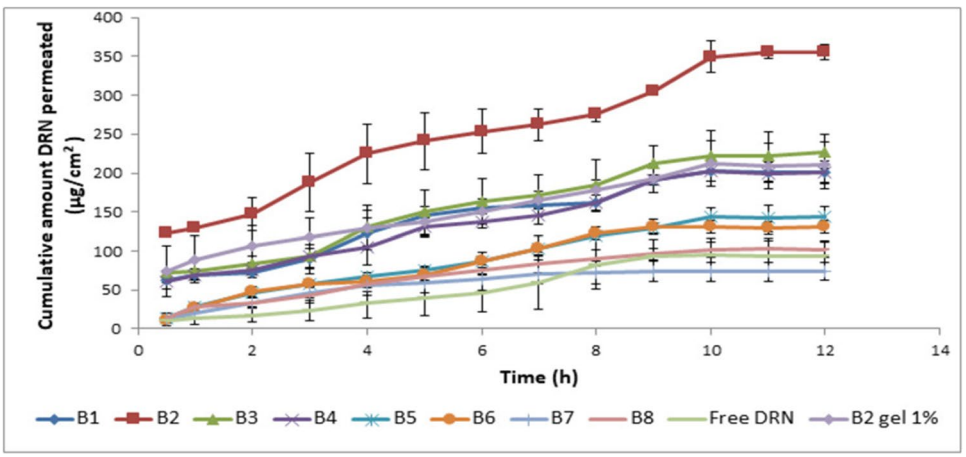

Fig. 2 Permeation plots of DRN from different bilosome formulae and B2 bilosomal gel compared to free drug suspension

and zwitter ionic surfactants [46]. Also, the presence of an edge activator (T60 or T80) reduces the stability of the bilosome membranes, hence escalating their elasticity and deformability by decreasing the interfacial tension [47]. This would convey a higher elastic nature to the formed bilosomes permitting them to squeeze in through fine skin pores and augment drug penetration across the skin [20].

At higher EA level, diffusion of the drug outside the nanovesicles into the dispersion medium may occur due to higher drug solubilization by formation of micelles or mixed micelles of small size which are able to release and permeate through the pores of the skin [25, 44, 48, 49].

Upon increasing PE content (X3), average flux (J_{12}) increased significantly. Our result is in accordance with that founded by Shen et al. [50] who achieved 2.4-fold enhanced blood level of ibuprofen after transdermal delivery of hydrogel containing clove oil as PE compared to control. The concept behind transdermal penetration enhancement of clove oil is that essential oils such as clove oil disrupt the highly ordered structure of stratum corneum lipids with concurrent increase of the intercellular diffusion [51, 52]. Beside,; high vesicle deformability acquired by increasing clove oil concentration resulted in enhanced skin permeation. Increasing the nanovesicles elasticity facilitates their squeezing through paracellular gap of narrow opening diameter. It also enables nanovesicles infiltration through the skin layers and diminishes the possibility of their rupture when squeezing [20, 32]. Furthermore; high lipophilicity of DRN may had a contributing mechanism of its skin penetration due to partitioning of lipophilic DRN into stratum corneum through intercellular spaces [51, 53].

Selection and Validation of the Optimal DRN-Loaded Bilosomes

The optimal formula from experimental design was B2 which fulfilled the predetermined conditions. High correlation was detected between the observed and predicted values of B2 (Table II). The average bias percent values for all the responses were smaller than 10%, confirming the high predictability of the implemented model [54]. B2 was chosen as the optimal formula for further studies.

TEM

TEM morphological photograph of the optimal formula B2 (Fig. 3) confirmed the spherical shape of vesicles and narrow size distribution. Vesicle size observed by TEM was in a good agreement with that measured by dynamic light scattering using Zetasizer.

In vitro Release Study of the Selected Formula

In vitro release profile showed enhanced cumulative % DRN released from bilosomal dispersion (B2) compared to free drug suspension as observed from release profile in Fig. 4. A similarity factor (f_2) value was 22.84. Similarity factor (f_2) value below 50 indicates that the compared formulae are not similar. Within 12 h, $70.29 \pm 6.46\%$ of DRN was released from bilosomal dispersion compared to only $13.3 \pm 1.2\%$ released from free drug suspension within the same period of time. The vast surface area of the formed nanovesicles and the incorporation of surfactants (T60 and SDC) enhanced DRN diffusion from the prepared bilosomes to the medium leading to a significant increase in DRN release rate and extent when compared to the free drug suspension.

DSC

The thermograms of pure DRN and lyophilized B2 are illustrated in Fig. 5. DRN showed a unique and well defined endothermic peak at 146.30°C, corresponding to its melting point, which suggests its purity and crystallinity. The enthalpy was found to be − 309.88 mJ/g. The DSC curve of B2 is observed at 102.88°C corresponding to its melting point, and the enthalpy was found to be − 38.04 mJ/g. The characteristic endothermic peak, corresponding to pure DRN melting was shifted towards lower temperature with lower peak intensity. The lower intensity of DRN peak in lyophilized B2 may be due to the solubilization of DRN

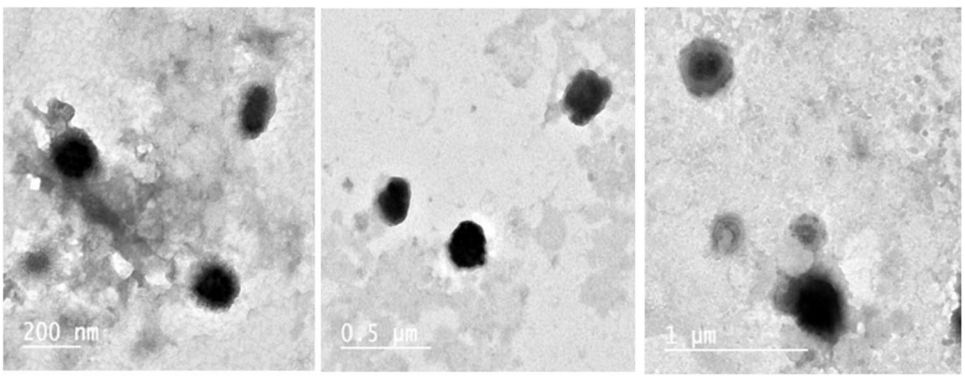

Fig. 3 TEM micrograph of the optimal formula B2

in the melted surfactants (SDC and T60) during heating as a result of their self-assembly into micelles in aqueous solution [55]. Also, the reduced intensity and broadening of DRN peaks with shifting towards lower temperature confirm the decrease of DRN crystallinity upon entrapment into bilosomes and/or drug solubilization in the EA surfactant as well as solid state interaction provoked by heating [55].

Stability Study of the Optimal Formula

After 90 days at 4°C and 25°C storage conditions, no visible aggregation or change was detected in stored bilosomes (B2). Retested VS, PDI, ZP, and EE% showed no significant difference from freshly prepared samples of B2. Stability results are summarized in Table 4. The negative charge of ZP was acquired from bile salt (SDC) which enhanced the ZP and prevent vesicles aggregation. Furthermore, the relatively high phase transition temperature (T_c) of Span® 40 (42°C) increases the tightness of the bilosome membrane and prohibits the drug leakage from vesicles and thus improves bilosomes stability [56]. In addition, the presence of nonionic surfactant EA (T60) could impart certain steric hindrance at bilosome membrane surface and maintained their stability.

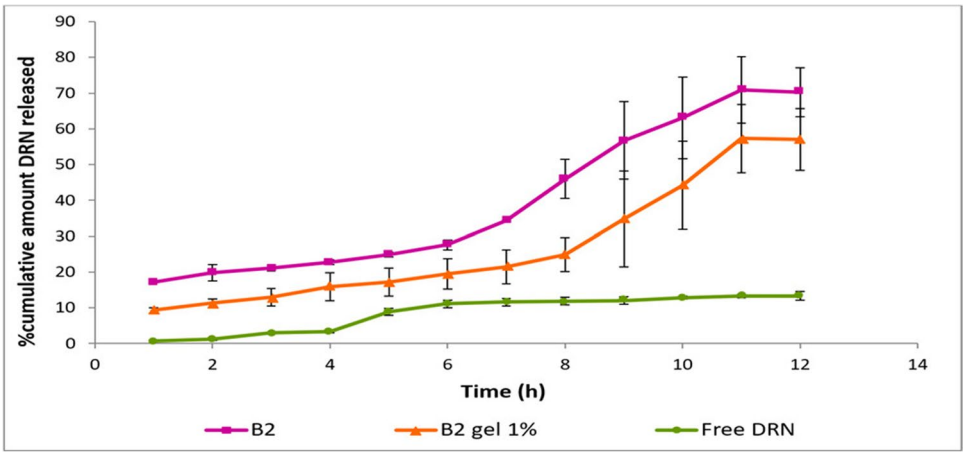

Fig. 4 Release profile of DRN from bilosomal dispersion B2 and bilosomal gel *vs.* free drug suspension

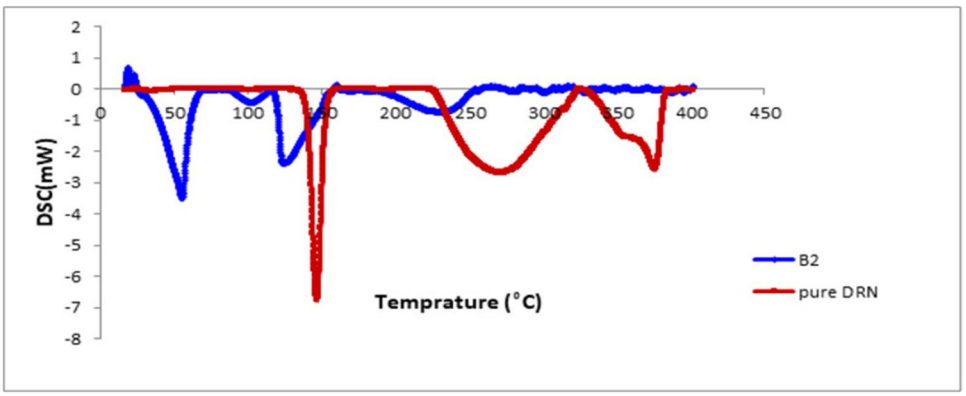

Fig. 5 DSC thermograms of pure DRN and lyophilized B2

Table 4 Effect of storage on physical stability of B2

Parameters	Freshly prepared	After 90 days at 4°C	After 90 days at 25°C	*P* value
VS (nm)	312.43 ± 24.4	311 ± 29.52	333.83 ± 29.69	0.566
PDI	0.54 ± 0.005	0.494 ± 0.03	0.53 ± 0.012	0.061
ZP (mV)	− 36.17 ± 2.57	− 34.57 ± 2.85	− 31.17 ± 1.21	0.093
EE %	80.95 ± 3.01	76.77 ± 3.63	78.6 ± 3.32	0.368

Data represented as mean ± SD ($n = 3$)

Evaluation of DRN Bilosomal Gel

Visual Examination and pH Measurements

The physical appearance of the B2 gel, the homogeneity, phase separation, and the color were investigated. A faint yellow color gel with the characteristic spicy and strong aroma of clove oil was observed. Gel was soft and smooth in texture without any grittiness and homogenous without any clumps, aggregates, or coarse particles. Homogenous appearance of the gel indicates that the bilosomal dispersion was uniformly distributed in the gel base and assures content uniformity and dose evenness. The faint yellow color is acquired from the clove oil in the formula. Gel was easily spreadable on the skin. No phase separation was observed. The pH value is an important factor for dermal formulations. The pH value of the bilosomal gel was 7.12 ± 0.3 which is close to the neutral pH (7.42–7.88) to prevent skin irritation [57, 58].

Viscosity Measurements and Rheological Properties

Viscosity is an essential aspect for semisolid formulations as it facilitates dermal application of the formulation and principally influences the drug diffusion and release from its carrier. The rheological behavior is also an indication for the in vivo retention after dermal application [59].

The prepared B2 loaded gel showed non-Newtonian psuedoplastic (shear thinning) flow with flow index (n) less than 1 as the viscosity was decreasing with increasing the shear rate (Fig. 6). This type of flow is much more beneficial to enhance the physical stability of bilosome dispersion; make dermal application easier upon shaking, pumping, or rubbing the gel; and to maintain gel retention after skin application [58].

In vitro Release Study of DRN-Loaded Bilosomal Gel

DRN-loaded bilosomal gel released $57.0 \pm 8.68\%$ of DRN within 12 h (Fig. 4). This decrease in % drug released compared to bilosomal dispersion indicates that the gelling agent has a delaying effect on the amount of DRN released. This effect may be due to acquired viscosity which acts as another diffusion barrier [60].

Ex vivo Permeation Study of DRN-Loaded Bilosomal Gel

B2 gel showed significantly lower Q10 (211.75 ± 29.43 µg/cm^2) and J_{12} (12.18 ± 1.67 µg/cm^2 h) compared to B2 bilosomes dispersion ($P < 0.05$). This might be due to increased bilosome dispersion viscosity which disturbed the drug diffusion to the release medium [61]. B2 dispersion and B2 gel showed an obvious higher DRN permeation in terms of rate and extent compared to the free drug suspension as illustrated in Fig. 2. Besides, the flux (J_{12}) values were estimated and the results showed significant difference ($P < 0.05$) between both B2 dispersion (21.23 ± 1.54 µg/cm^2 h) and B2 gel formula (12.18 ± 1.67 µg /cm^2 h) compared to free drug suspension (6.61 ± 1.85 µg /cm^2 h). Furthermore; ER values of B2 dispersion and B2 gel were found to be 3.2 and 1.85, respectively; verifying the significant enhancement of DRN permeation across skin. These results might be attributed to the combined effects of nanosized vesicles, vesicle elasticity imparted by the presence of edge activator, and the presence of clove oil as permeation enhancer which facilitates their skin penetration.

Ex vivo Skin Deposition Study of DRN-Loaded Bilosomal Gel

Amount of DRN deposited from bilosomal gel into different rats' skin layers were found to be 362.12 ± 56.93 µg in stratum corneum, 123.7 ± 56.90 µg in epidermis layer, and 86.5 ± 50.7 µg in dermis layer. DRN deposition into different skin layers is obviously due to high deformability of

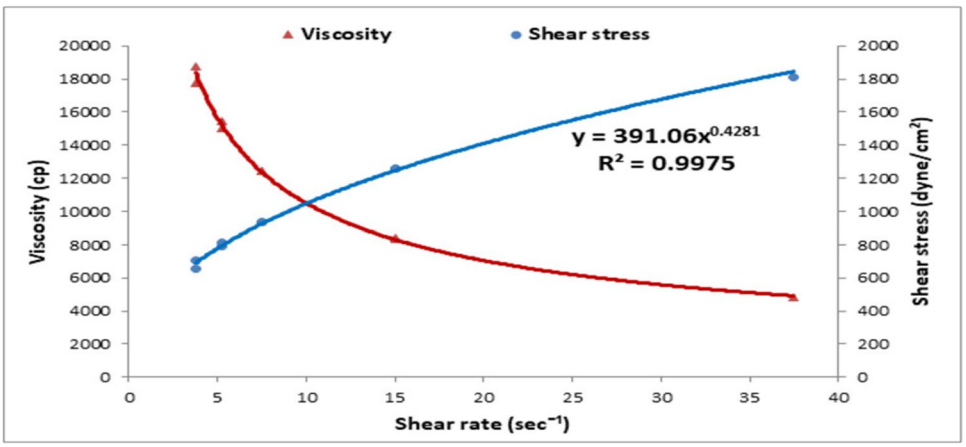

Fig. 6 Rheological behavior of the prepared bilosomal gel

DRN bilosomes which could squeeze through paracellular gap of different skin tissues. Furthermore, skin deposition of DRN-loaded bilosomes could be attributed to the chemical interaction of anionic head group of SDC (bile salt) in the bilosomes with cationic region of skin proteins [62]. Increased DRN deposition into skin layers might be a good precursor of enhanced transdermal flux.

Conclusion

In the present study, bilosomes were developed for transdermal delivery of DRN for enhancement of its skin flux and permeability. A 2^3 full-factorial experimental design was utilized for selecting optimal formula (B2) that showed small VS, high drug EE%, and good stability. Ex vivo studies revealed superior DRN permeation from B2 over free DRN suspension. B2 was incorporated into gel base for ease of dermal application. Transdermal gel formulation showed good and acceptable physical characteristics, non-Newtonian psuedoplastic flow and manifestly higher DRN release and skin permeability compared to free drug suspension. Finally, the results verified the aptitude of B2 to be a probable TDDS for DRN through eradication of its extensive first-pass metabolism when administered orally.

Author Contribution Study design, experimental work, data analysis, results interpretation and manuscript writing: Jihad Mahmoud Alsofany. Orientation, revision, and corrections: Mahmoud H. Teaima and Mohamed A. El-Nabarawi. All authors have approved the submitted final version.

Funding Open access funding provided by The Science, Technology & Innovation Funding Authority (STDF) in cooperation with The Egyptian Knowledge Bank (EKB).

Declarations

Conflict of Interest The authors declare no competing interests.

References

1. Doggrell SA, Hancox JC. Dronedarone: an amiodarone analogue. Expert Opin Investig Drugs. 2005;13(4):415–26. https://doi.org/10.1517/13543784.13.4.415.
2. Gambhire VM, Gambhire MS, Ranpise NS. Solid lipid nanoparticles of dronedarone hydrochloride for oral delivery: optimization, in vivo pharmacokinetics and uptake studies. Pharmaceutical Nanotechnology. 2019;7(5):375–88. https://doi.org/10.2174/2211738507666190802140607.
3. Jung HJ, Han SD, Kang MJ. Enhanced dissolution rate of dronedarone hydrochloride via preparation of solid dispersion using vinylpyrrolidone-vinyl acetate copolymer (Kollidone® VA 64). Bull Korean Chem Soc. 2015;36(9):2320–4. https://doi.org/10.1002/bkcs.10455.
4. Han SD, Jung SW, Jang SW, Son M, Kim BM, Kang MJ. Reduced food-effect on intestinal absorption of dronedarone by self-microemulsifying drug delivery system (SMEDDS). Biol Pharm Bull. 2015;38(7):1026–32.
5. Sguizzato M, Esposito E, Cortesi R. Lipid-based nanosystems as a tool to overcome skin barrier. Int J Mol Sci. 2021;22(15):8319. https://doi.org/10.3390/ijms22158319.
6. Singh D, Pradhan M, Nag M, Singh MR. Vesicular system: versatile carrier for transdermal delivery of bioactives. Artificial Cells, Nanomedicine, and Biotechnology. 2014;43(4):282–90. https://doi.org/10.3109/21691401.2014.883401.
7. Honeywell-Nguyen PL, Bouwstra JA. Vesicles as a tool for transdermal and dermal delivery. Drug Discov Today Technol. 2005;2(1):67–74. https://doi.org/10.1016/j.ddtec.2005.05.003.
8. Marcolino AIP, Macedo LB, Nogueira-Librelotto DR, Fernandes JR, Bender CR, Wust KM, et al. Preparation, characterization and in vitro cytotoxicity study of dronedarone hydrochloride inclusion complexes. Mater Sci Eng, C. 2019;100:48–61. https://doi.org/10.1016/j.msec.2019.02.097.
9. Mahapatra AK, Samoju S, Patra RK, Murthy PN. Dissolution enhancement of dronedarone hydrochloride by complexation with β-CD and HP β-CD: dissolution and physicochemical characterization. 2014.
10. Kovvasu SP, Kunamaneni P, Yeung S, Rueda J, Betageri GV. Formulation of dronedarone hydrochloride-loaded proliposomes: in vitro and in vivo evaluation using Caco-2 and rat model. AAPS PharmSciTech. 2019;20(6). https://doi.org/10.1208/s12249-019-1437-5.
11. Conacher M, Alexander J, Brewer JM. Oral immunisation with peptide and protein antigens by formulation in lipid vesicles incorporating bile salts (bilosomes). Vaccine. 2001;19(20–22):2965–74.
12. Cui M, Wu W, Hovgaard L, Lu Y, Chen D, Qi J. Liposomes containing cholesterol analogues of botanical origin as drug delivery systems to enhance the oral absorption of insulin. Int J Pharm. 2015;489(1–2):277–84. https://doi.org/10.1016/j.ijpharm.2015.05.006.
13. El-Nabarawi MA, Shamma RN, Farouk F, Nasralla SM. Bilosomes as a novel carrier for the cutaneous delivery for dapsone as a potential treatment of acne: preparation, characterization and in vivo skin deposition assay. J Liposome Res. 2019;30(1):1–11. https://doi.org/10.1080/08982104.2019.1577256.
14. Sallam N, Sanad R, KHAFAGY E-S, Ahmed M, Ghourab M, Gad S. Colloidal delivery of drugs: present strategies and conditions. Records of Pharmaceutical and Biomedical Sciences. 2021;5(Pharmacology-Pharmaceutics):40–51. https://doi.org/10.21608/rpbs.2020.30372.1070.
15. Kesarwani K, Gupta R. Bioavailability enhancers of herbal origin: An overview. Asian Pac J Trop Biomed. 2013;3(4):253–66. https://doi.org/10.1016/s2221-1691(13)60060-x.

16. Bashyal S, Seo J-E, Keum T, Noh G, Choi YW, Lee S. Facilitated permeation of insulin across TR146 cells by cholic acid derivatives-modified elastic bilosomes. Int J Nanomed. 2018;13:5173–86. https://doi.org/10.2147/ijn.s168310.
17. Ahmed S, Kassem MA, Sayed S. Bilosomes as promising nanovesicular carriers for improved transdermal delivery: construction, in vitro optimization, ex vivo permeation and in vivo evaluation. Int J Nanomedicine. 2020;15:9783–98.
18. Aziz DE, Abdelbary AA, Elassasy AI. Investigating superiority of novel bilosomes over niosomes in the transdermal delivery of diacerein: in vitro characterization, ex vivo permeation and in vivo skin deposition study. J Liposome Res. 2018;29(1):73–85. https://doi.org/10.1080/08982104.2018.1430831.
19. Al-mahallawi AM, Abdelbary AA, Aburahma MH. Investigating the potential of employing bilosomes as a novel vesicular carrier for transdermal delivery of tenoxicam. Int J Pharm. 2015;485(1–2):329–40. https://doi.org/10.1016/j.ijpharm.2015.03.033.
20. Kakkar S, Kaur IP. Spanlastics—a novel nanovesicular carrier system for ocular delivery. Int J Pharm. 2011;413(1–2):202–10. https://doi.org/10.1016/j.ijpharm.2011.04.027.
21. Abdelbary AA, Abd-Elsalam WH, Al-mahallawi AM. Fabrication of novel ultradeformable bilosomes for enhanced ocular delivery of terconazole: in vitro characterization, ex vivo permeation and in vivo safety assessment. Int J Pharm. 2016;513(1–2):688–96. https://doi.org/10.1016/j.ijpharm.2016.10.006.
22. El Zaafarany GM, Awad GAS, Holayel SM, Mortada ND. Role of edge activators and surface charge in developing ultradeformable vesicles with enhanced skin delivery. Int J Pharm. 2010;397(1–2):164–72. https://doi.org/10.1016/j.ijpharm.2010.06.034.
23. Lei W, Yu C, Lin H, Zhou X. Development of tacrolimus-loaded transfersomes for deeper skin penetration enhancement and therapeutic effect improvement in vivo. Asian J Pharm Sci. 2013;8(6):336–45. https://doi.org/10.1016/j.ajps.2013.09.005.
24. Gupta PN, Mishra V, Rawat A, Dubey P, Mahor S, Jain S, et al. Non-invasive vaccine delivery in transfersomes, niosomes and liposomes: a comparative study. Int J Pharm. 2005;293(1–2):73–82. https://doi.org/10.1016/j.ijpharm.2004.12.022.
25. Fahmy AM, El-Setouhy DA, Habib BA, Tayel SA. Enhancement of transdermal delivery of haloperidol via spanlastic dispersions: entrapment efficiency vs. particle size. AAPS PharmSciTech. 2019;20(3). https://doi.org/10.1208/s12249-019-1306-2.
26. Fahmy AM, El-Setouhy DA, Ibrahim AB, Habib BA, Tayel SA, Bayoumi NA. Penetration enhancer-containing spanlastics (PECSs) for transdermal delivery of haloperidol: in vitro characterization, ex vivo permeation and in vivo biodistribution studies. Drug Delivery. 2017;25(1):12–22. https://doi.org/10.1080/10717544.2017.1410262.
27. Kim JK, Zeb A, Qureshi OS, Kim H-S, Cha J-H, Kim H-S. Improved skin permeation of methotrexate via nanosized ultradeformable liposomes. Int J Nanomed. 2016;11:3813–24. https://doi.org/10.2147/ijn.s109565.
28. Surber C, Schwarb FP, Smith EW. Tape-stripping technique. Journal of Toxicology: Cutaneous and Ocular Toxicology. 2001;20(4):461–74. https://doi.org/10.1081/cus-120001870.
29. Verma DD, Verma S, Blume G, Fahr A. Particle size of liposomes influences dermal delivery of substances into skin. Int J Pharm. 2003;258(1–2):141–51.
30. Cho HJ, Park JW, Yoon IS, Kim DD. Surface-modified solid lipid nanoparticles for oral delivery of docetaxel: enhanced intestinal absorption and lymphatic uptake. Int J Nanomedicine. 2014;9:495–504.
31. Danaei M, Dehghankhold M, Ataei S, Hasanzadeh Davarani F, Javanmard R, Dokhani A, et al. Impact of particle size and polydispersity index on the clinical applications of lipidic nanocarrier systems. Pharmaceutics. 2018;10(2).
32. Elsayed I, El-Dahmy RM, El-Emam SZ, Elshafeey AH, El Gawad NAA, El-Gazayerly ON. Response surface optimization of biocompatible elastic nanovesicles loaded with rosuvastatin calcium: enhanced bioavailability and anticancer efficacy. Drug Deliv Transl Res. 2020;10(5):1459–75. https://doi.org/10.1007/s13346-020-00761-0.
33. ElMeshad AN, Mohsen AM. Enhanced corneal permeation and antimycotic activity of itraconazole against Candida albicans via a novel nanosystem vesicle. Drug Delivery. 2014;23(7):2115–23. https://doi.org/10.3109/10717544.2014.942811.
34. Mazyed EA, Helal DA, Elkhoudary MM, AbdElhameed AG, Yasser M. Formulation and optimization of nanospanlastics for improving the bioavailability of green tea epigallocatechin gallate. Pharmaceuticals. 2021;14(1):68. https://doi.org/10.3390/ph14010068.
35. Ruckmani K, Sankar V. Formulation and optimization of zidovudine niosomes. AAPS PharmSciTech. 2010;11(3):1119–27. https://doi.org/10.1208/s12249-010-9480-2.
36. Hao Y-M, Li Ka. Entrapment and release difference resulting from hydrogen bonding interactions in niosome. International Journal of Pharmaceutics. 2011;403(1–2):245–53. https://doi.org/10.1016/j.ijpharm.2010.10.027.
37. Wang N, Hsu C, Zhu L, Tseng S, Hsu JP. Influence of metal oxide nanoparticles concentration on their zeta potential. J Colloid Interface Sci. 2013;407:22–8.
38. Lee EH, Kim A, Oh Y-K, Kim C-K. Effect of edge activators on the formation and transfection efficiency of ultradeformable liposomes. Biomaterials. 2005;26(2):205–10. https://doi.org/10.1016/j.biomaterials.2004.02.020.
39. Yang T, Cui F-D, Choi M-K, Cho J-W, Chung S-J, Shim C-K, et al. Enhanced solubility and stability of PEGylated liposomal paclitaxel: in vitro and in vivo evaluation. Int J Pharm. 2007;338(1–2):317–26. https://doi.org/10.1016/j.ijpharm.2007.02.011.
40. Tayel SA, El-Nabarawi MA, Tadros MI, Abd-Elsalam WH. Duodenum-triggered delivery of pravastatin sodium via enteric surface-coated nanovesicular spanlastic dispersions: Development, characterization and pharmacokinetic assessments. Int J Pharm. 2015;483(1–2):77–88. https://doi.org/10.1016/j.ijpharm.2015.02.012.
41. Wilson B, Samanta MK, Santhi K, Kumar KPS, Paramakrishnan N, Suresh B. Poly(n-butylcyanoacrylate) nanoparticles coated with polysorbate 80 for the targeted delivery of rivastigmine into the brain to treat Alzheimer's disease. Brain Res. 2008;1200:159–68. https://doi.org/10.1016/j.brainres.2008.01.039.
42. Huang Y-B, Tsai M-J, Wu P-C, Tsai Y-H, Wu Y-H, Fang J-Y. Elastic liposomes as carriers for oral delivery and the brain distribution of (+)-catechin. J Drug Target. 2011;19(8):709–18. https://doi.org/10.3109/1061186x.2010.551402.
43. Xue Y, Zhou S, Fan C, Du Q, Jin P. Enhanced antifungal activities of eugenol-entrapped casein nanoparticles against anthracnose in postharvest Fruits. Nanomaterials. 2019;9(12):1777. https://doi.org/10.3390/nano9121777.
44. van den Bergh BA, Wertz PW, Junginger HE, Bouwstra JA. Elasticity of vesicles assessed by electron spin resonance, electron microscopy and extrusion measurements. Int J Pharm. 2001;217(1–2):13–24. https://doi.org/10.1016/s0378-5173(01)00576-2.
45. Elsayed I, El-Dahmy RM, Elshafeey AH, Abd El Gawad NA, El Gazayerly ON. Tripling the bioavailability of rosuvastatin calcium through development and optimization of an in-situ forming nanovesicular system. Pharmaceutics. 2019;11(6):275. https://doi.org/10.3390/pharmaceutics11060275.
46. Shabbir M, Ali S, Farooq M, Adnan S, Yousaf M, Idrees A, et al. Formulation factors affecting in vitro and ex vivo permeation of

bisoprolol fumarate from a matrix transdermal patch. Adv Polym Technol. 2016;35(3):237–47. https://doi.org/10.1002/adv.21546.
47. Trotta M, Peira E, Debernardi F, Gallarate M. Elastic liposomes for skin delivery of dipotassium glycyrrhizinate. Int J Pharm. 2002;241(2):319–27. https://doi.org/10.1016/s0378-5173(02)00266-1.
48. Basha M, Abd El-Alim SH, Shamma RN, Awad GEA. Design and optimization of surfactant-based nanovesicles for ocular delivery of Clotrimazole. J Liposome Res. 2013;23(3):203–10. https://doi.org/10.3109/08982104.2013.788025.
49. Salama HA, Mahmoud AA, Kamel AO, Abdel Hady M, Awad GAS. Brain delivery of olanzapine by intranasal administration of transfersomal vesicles. J Liposome Res. 2012;22(4):336–45. https://doi.org/10.3109/08982104.2012.700460.
50. Shen Q, Li W, Li W. The effect of clove oil on the transdermal delivery of ibuprofen in the rabbit by in vitro and in vivo methods. Drug Dev Ind Pharm. 2007;33(12):1369–74. https://doi.org/10.1080/03639040701399346.
51. Chen J, Jiang Q-D, Wu Y-M, Liu P, Yao J-H, Lu Q, et al. Potential of essential oils as penetration enhancers for transdermal administration of ibuprofen to treat dysmenorrhoea. Molecules. 2015;20(10):18219–36. https://doi.org/10.3390/molecules201018219.
52. Parhi R, Suresh P, Mondal S, Kumar PM. Novel penetration enhancers for skin applications: a review. Curr Drug Deliv. 2012;9(2):219–30.
53. Jiang Q, Wu Y, Zhang H, Liu P, Yao J, Yao P, et al. Development of essential oils as skin permeation enhancers: penetration enhancement effect and mechanism of action. Pharm Biol. 2017;55(1):1592–600. https://doi.org/10.1080/13880209.2017.1312464.
54. Abdel-Hafez SM, Hathout RM, Sammour OA. Tracking the transdermal penetration pathways of optimized curcumin-loaded chitosan nanoparticles via confocal laser scanning microscopy. Int J Biol Macromol. 2018;108:753–64. https://doi.org/10.1016/j.ijbiomac.2017.10.170.
55. Adibkia K, Javadzadeh Y, Dastmalchi S, Mohammadi G, Niri FK, Alaei-Beirami M. Naproxen–eudragit® RS100 nanoparticles: preparation and physicochemical characterization. Colloids Surf, B. 2011;83(1):155–9. https://doi.org/10.1016/j.colsurfb.2010.11.014.
56. Vora B, Khopade AJ, Jain NK. Proniosome based transdermal delivery of levonorgestrel for effective contraception. J Control Release. 1998;54(2):149–65.
57. Aiyalu R, Govindarjan A, Ramasamy A. Formulation and evaluation of topical herbal gel for the treatment of arthritis in animal model. Braz J Pharm Sci. 2016;52(3):493–507. https://doi.org/10.1590/s1984-82502016000300015.
58. Oktay AN, Ilbasmis-Tamer S, Han S, Uludag O, Celebi N. Preparation and in vitro / in vivo evaluation of flurbiprofen nanosuspension-based gel for dermal application. Eur J Pharm Sci. 2020;155:105548. https://doi.org/10.1016/j.ejps.2020.105548.
59. Abdelrahman FE, Elsayed I, Gad MK, Elshafeey AH, Mohamed MI. Response surface optimization, ex vivo and in vivo investigation of nasal spanlastics for bioavailability enhancement and brain targeting of risperidone. Int J Pharm. 2017;530(1–2):1–11.
60. Garhy DMA, Ismail S, Ibrahim HK, Ghorab MM. Buccoadhesive gel of carvedilol nanoparticles for enhanced dissolution and bioavailability. Journal of Drug Delivery Science and Technology. 2018;47:151–8. https://doi.org/10.1016/j.jddst.2018.07.009.
61. Zare-Akbari Z, Farhadnejad H, Furughi-Nia B, Abedin S, Yadollahi M, Khorsand-Ghayeni M. PH-sensitive bionanocomposite hydrogel beads based on carboxymethyl cellulose/ZnO nanoparticle as drug carrier. Int J Biol Macromol. 2016;93(Pt A):1317–27.
62. Som I, Bhatia K, Yasir M. Status of surfactants as penetration enhancers in transdermal drug delivery. J Pharm Bioallied Sci. 2012;4(1):2–9.